Politecnico di Torino

Corso di Laurea Magistrale in
Ingegneria Chimica e dei processi sostenibili

Master Thesis

Development of membranes for hydrogen fuel cells and electrolyzers for hydrogen production

Supervisor:

Prof. Bocchini Sergio

Candidate:

Iacovino Vincenzo

October 2023

Index

Figure Index

Table Index

Legend

PIM: Intrinsically microporous polymers

cPIM: Carboxylate PIM

PEMFC: Polymer electrolyte membrane fuel cells

MEA: Membrane electrode assembly

SBI: Spirobisindane

PBI: Polybenzimidazole

IR: Infrared Analysis

DSC: Differential Scanning Calorimetry

TGA: Thermogravimetric Analysis

ATR: Attenuated Total Reflection

DVS: Dynamic Vapor Sorption

DMF: Dimethyformamide

DMSO: Dimethyl sulfoxide

SPIRO: 5,5′,6,6′-tetrahydroxy-3,3,3′,3′-tetramethyl-1,1′-spirobisindane

TFTCN: Tetrafluoroterephthalonitrile

THF: Tetrahydrofuran

NMP: N-Methyl-2-pyrrolidone

Introduction

With this thesis, we embark on a study within a field of growing importance, aimed at addressing the challenges related to the sustainable production of hydrogen, a crucial element for the future of clean energy. This master's thesis aims to explore and analyse in detail the use of proton exchange membranes, fundamental tools for the selective transport of ions, particularly protons (H^+), in the context of hydrogen production.

In the first section of this thesis, we provide a comprehensive overview of the importance of hydrogen as an increasingly relevant energy carrier, delving into the main mechanisms for its production. Subsequently, we discuss the evolution in the field of membranes used for hydrogen transport, highlighting the obsolescence of Nafion-based membranes and the introduction of membranes based on intrinsically microporous polymers (PIM) as an innovative alternative.

In the second section of the thesis, we will present the tools used during my experience at the Italian Institute of Technology in Turin, along with details of the analytical methods employed for the synthesis of various polymers.

The following chapter will delve into all phases of the process in detail, offering a critical analysis of the results obtained. Chapters four and five will be dedicated to illustrating the key steps for the production of membranes based on the new polymer developed. Finally, in the concluding chapter, the entire research journey will be synthesized, highlighting the results achieved and sharing reflections arising from my experience within the research team.

This thesis represents a significant contribution to the field of sustainable hydrogen production, and I am confident that it can inspire further research and developments in this crucial area for the future of our planet.

1 Hydrogen Production: From Nafion Membranes to Intrinsic Microporous Polymers

1.1 Hydrogen: Energy transition, production and consumption

In the current global energy context, the search for sustainable and efficient energy sources has become a crucial objective in addressing challenges related to climate change and energy security. In this context, hydrogen emerges as a promising alternative, both as a clean fuel and as a versatile energy carrier.

Its high energy density and the potential for production from renewable sources make it a candidate of significant interest for the transition to a low-carbon economy. [1] From an electrochemical perspective, the production and consumption of hydrogen using proton exchange membranes appear as a promising strategy. Proton exchange membranes play a pivotal role in numerous applications, including polymer electrolyte membrane fuel cells (PEMFCs), a system that embodies the future of sustainable energy production.

1.2 Proton Exchange Membrane Fuel Cell - PEMFC

Fuel cells are electrochemical devices that exploit the direct conversion of the chemical energy from a fuel, such as hydrogen, into electrical energy. Unlike traditional thermal systems, they do not involve intermediate thermal cycles, allowing for significantly higher conversion efficiencies.

The most widespread and widely recognized type is the Proton Exchange Membrane Fuel Cell (PEMFC). PEMFCs employ a proton-conductive membrane, which serves both as an electrolyte and a separator within the electrochemical cell.

This membrane, pivotal for PEMFCs, is renowned for its high efficiency in proton conduction, enabling optimal electrical reactivity. These devices operate through electrochemical processes, necessitating the continuous presence of fuel (hydrogen) and an oxidizing agent (oxygen or air) to generate electrical power.

In other words, a fuel cell does not store energy but rather converts it as long as reactants are available. The fundamental structure of a PEMFC, Figure 1, comprises two bipolar plates separated by the Membrane Electrode Assembly (MEA). The MEA consists of a highly proton-conductive polymeric membrane, two porous electrodes typically equipped with platinum-based catalysts, and two gas diffusion layers (GDLs).

These high-quality materials facilitate a uniform distribution of reactants along the membrane, ensuring optimal reaction efficiency.

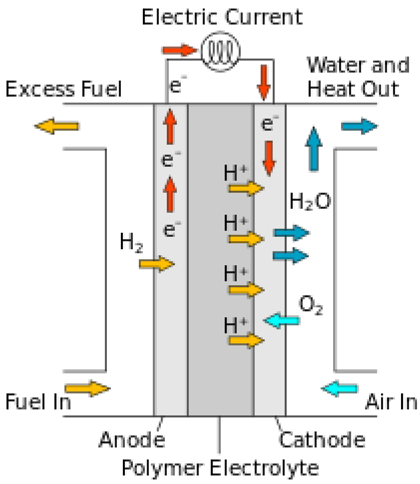

Figure 1 -Example of how a PEMFC works.

In detail, the flow of hydrogen is directed to the anodic side, where the oxidation reaction of hydrogen takes place:

$$H_2 \rightarrow 2\,H^+ + 2\,e^-$$

This process allows hydrogen ions (protons) to pass through the membrane to the anode, while electrons follow an external path, generating the fuel cell current that powers the connected load until it reaches the cathodic side.

Meanwhile, oxygen flow is supplied to the cathode, where oxygen molecules react with the protons and electrons from the external circuit. This process leads to the formation of water molecules through the oxygen reduction reaction.

$$\frac{1}{2} O_2 + 2 H^+ + 2e^- \rightarrow H_2O$$

Proton exchange membranes offer numerous advantages, including high electrochemical conversion efficiency, absence of harmful emissions, and adaptability to both stationary and mobile applications. However, as with any technology, there are also some challenges associated with the use of proton exchange membranes.

Among the main drawbacks are their sensitivity to impurities in the feed gases, the high cost of materials used in their production, and the need to maintain optimal humidity conditions for their operation. [2] [3] [4] [5] [6]

1.3 Nafion membrane

From an electrochemical perspective, the production and consumption of hydrogen using proton exchange membranes appear as a promising strategy.

Proton exchange membranes play a fundamental role in numerous applications, including polymer electrolyte membrane fuel cells

(PEMFCs), a system that embodies the future of sustainable energy production. In PEMFCs, water is supplied to the cell, and an electrical potential is applied. This process allows hydrogen ions (protons) to cross the membrane toward the anode, while oxygen ions move towards the cathode. This precise and controlled ionic separation enables the selective extraction of hydrogen ions, which can be collected as pure hydrogen gas. Proton exchange membranes offer several advantages, including high electrochemical conversion efficiency, absence of harmful emissions, and adaptability to both stationary and mobile applications.

However, like any technology, there are also challenges associated with the use of proton exchange membranes. Among the main drawbacks are their sensitivity to impurities in the feed gases, the high cost of materials used in their production, and the need to maintain optimal humidity conditions for their operation. [7] However, there are some challenges associated with its chemical structure characterized by the presence of fluorine and sulphur atoms. Among the key advantages of Nafion are high proton transfer efficiency, chemical and mechanical stability in corrosive environments, and its ability to operate within an acceptable range of temperature and humidity. Nevertheless, its use also comes with certain limitations.

The fluorine content, while imparting Nafion with high hydrophobic and chemical resistance properties, makes the polymer expensive to produce and manage at the end of its lifecycle due to the poor biodegradability of fluorinated compounds. [8]

This complexity in the chemical structure of Nafion, Figure 2, has driven research to explore alternative materials that can compete with Nafion's effectiveness while addressing the issues related to fluorine and sulphur.

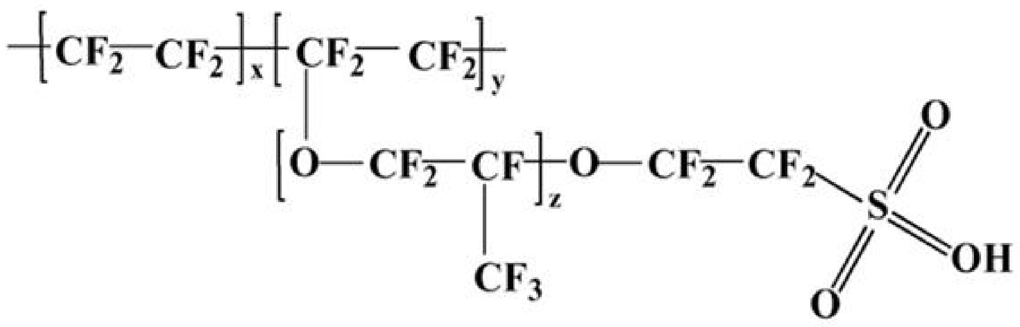

Figure 2-Chemical structure of Nafion

1.4 Innovative Membranes with Intrinsically Microporous Polymers: PIM

In this perspective, Intrinsically Microporous Polymers (PIMs), coined by Budd and Neil B. McKeown, emerge as a promising alternative. [9] According to the sources cited, Intrinsically Microporous Polymers (PIMs), Figure 3, constitute a category of macromolecules with unique properties and distinctive chemical structures. The IUPAC definition of micropores identifies pores with a diameter less than 20 nm, which imparts to them a high surface area of 1000 m²/g.

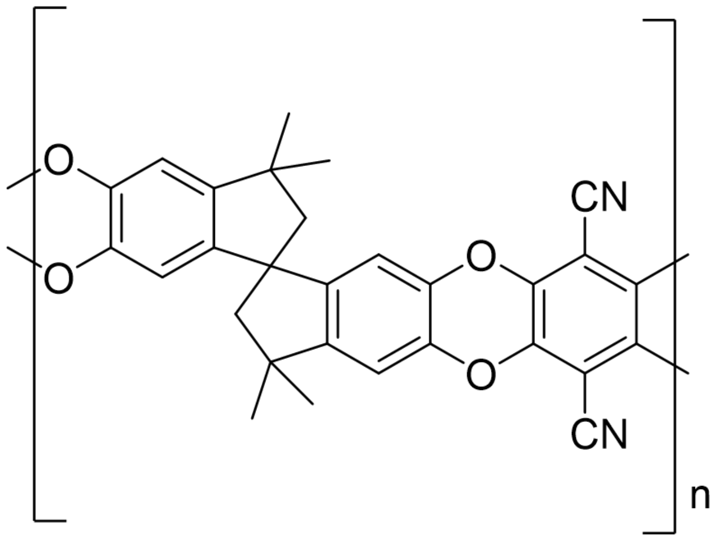

Figure 3-Chemical structure of polymer PIM1

Additionally, Intrinsically Microporous Polymers (PIMs) are comprised of two distinct components: a structural unit that possesses concavities, introducing points of contortion into the polymer chain, and, secondly, a linking group (such as benzodioxin) that connects the structural units during polymerization, limiting rotation and conferring molecular rigidity while facilitating solvent access into the polymer solid, aiding in dissolution. [10] [11]

PIM1 is a polymer consisting of a structural unit known as spirobisindane (SBI), while the linking group is precisely benzodioxin. Membranes based on PIM-1 find applications in various sectors, with a significant impact in technologies that leverage its selective capabilities towards various substances. They prove advantageous in areas such as CO_2 capture, water treatment, and solvent recovery. [12] [13] [14] [15]

1.5 Development of new membrane

In this thesis, a study based on the robust theory of PIM-1 was undertaken. The research team, comprised of distinguished members including Professor Bocchini S., Ferraro G., Bartoli M., Lettieri S., De Nardo E., and Astorino C., focused their attention on the excellent characteristics of Polybenzimidazole (PBI). They replaced the -CN functional groups in the main chain of PIM-1 with benzimidazole functional groups. PBI, as also described in the cited articles, emerges as a polymer of significant relevance in high-temperature proton exchange membranes. Particularly, PBI is renowned for its high thermal and chemical stability, as well as its resistance to acids and corrosion. These attributes are essential to ensure the integrity and durability of membranes in contexts such as fuel cells. Furthermore, PBI demonstrates good proton conductivity even at elevated temperatures, enhancing the efficiency of electrochemical reactions. All these characteristics, conferred by the benzimidazole group of the polymer, form the basis of the central objective of this thesis: to combine the distinctive properties of PIM-1 with those of PBI by creating a polymer that possesses the central structure of PIM-1 enriched with benzimidazole functional groups. [16] [17] [18]

The subsequent objective is the development of a new material, known as Benzimidazol-PIM, which could potentially exhibit a unique set of properties synthesized from the interaction of these two polymer components.

2 Materials and Methods

This chapter provides a detailed account of the materials, methods, and procedures used in the research to evaluate and validate the obtained results. It covers information about the materials, experimental procedures, and analytical techniques employed in investigating and characterizing the polymers. This encompasses details about the source and properties of starting materials, including chemical reagents, existing polymers, and catalysts. The specifications of equipment and instruments utilized in polymer synthesis will also be outlined. The evaluation of physical and chemical properties will be conducted through various analyses such as Infrared Analysis (IR), Differential Scanning Calorimetry (DSC), Thermogravimetric Analysis (TGA), and other characterization techniques, all of which will be elaborated. This chapter provides a comprehensive insight into the materials, procedures, and methodologies applied throughout the research.

2.1 Techniques and analysis

2.1.1 AT-IR Spectroscopy theory

Attenuated Total Reflection (ATR) IR Spectroscopy is a widely used analytical technique in the scientific field for studying the molecular composition of materials.

This technique is based on infrared (IR) spectroscopy, which is a non-destructive and highly sensitive method of chemical analysis used to identify various molecular species in a sample.

ATR IR Spectroscopy exploits the phenomenon of attenuated total reflection, which occurs when infrared light is directed onto a material with a high refractive index, such as a crystal with a reflective inner surface. When the light beam passes through the sample material, some of the energy is absorbed by the molecules present at the contact surface between the crystal and the sample.

This leads to the creation of a unique infrared absorption spectrum for the analysed sample. Practically, the sample is simply pressed against the surface of the crystal, and the interaction between the infrared light and the sample occurs at a very shallow depth (typically a few microns) from the surface.

This makes ATR IR Spectroscopy ideal for analysing solid, liquid, and pasty samples without the need for complex sample preparations. [19] [20] [21]

2.1.2 AT-IR spectroscopy

Each sample was analysed using a Bruker Invenio spectrometer equipped with a deuterated triglycine sulphate (DTGS) detector and the Bruker Platinum attenuated total reflection (ATR) accessory with a diamond crystal. Infrared spectra were recorded by averaging 24 scans with a resolution of 4 cm^{-1} in the spectral range from 4500 to 400 cm^{-1} for both the background and the sample.

2.1.3 TGA-IR analysis theory

TGA-IR (Thermogravimetric Analysis-Infrared) analysis is an advanced analytical technique that combines thermogravimetry (TGA) with infrared spectroscopy (IR).

This technique is widely used in the scientific field to study the chemical composition and thermal properties of materials. TGA is a technique that measures the change in mass of a sample as a function of temperature.

During TGA analysis, the sample is gradually heated while its loss of mass is monitored. This information is useful for determining the content of water, solvents, plasticizers, or other volatile species present in the sample, as well as for studying decomposition reactions, degradation, or general mass loss. In TGA-IR analysis, infrared spectroscopy is used in combination with TGA to acquire IR spectra of the sample at specific critical points of the thermogravimetric curve. These points may include regions of maximum mass loss, transition temperatures, or specific events relevant to the material under examination. [22] [23] [24]

2.1.4 Thermo-gravimetric analysis coupled with IR gas analysis (TGA-IR)

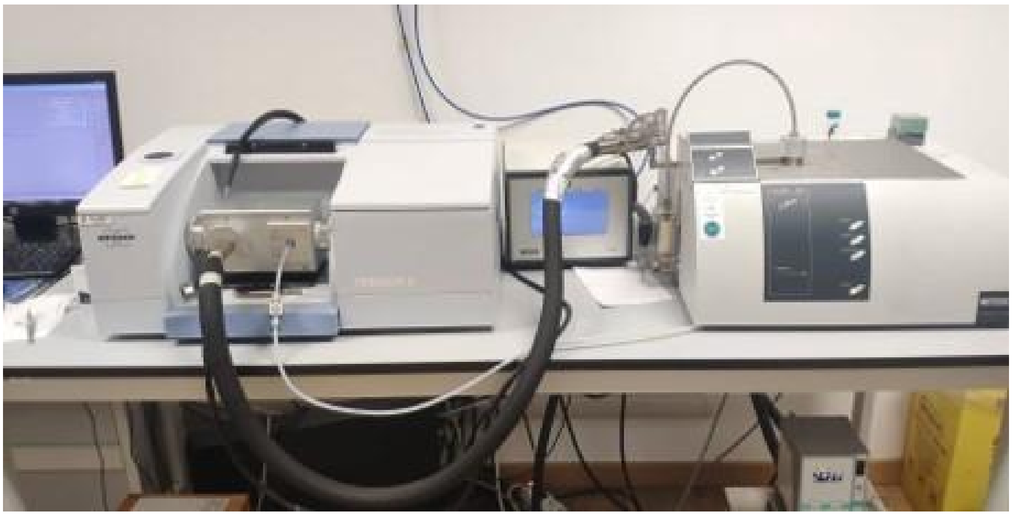

Figure 4-Picture of TGA-IR instrument

Thermogravimetric measurements and infrared gas analysis were conducted. TG measurements were performed using a Netzsch TG 209 F1 Libra thermogravimetric analyser (Figure 4). In the crucible, a sample quantity between 5 and 10 mg was placed and heated from 30°C to 800°C at a rate of 10°C/min under a flow of 40 ml/min of nitrogen. The gases produced were analysed using a Bruker infrared spectrometer coupled with a heated transfer line.

2.1.5 DSC analysis theory

DSC (Differential Scanning Calorimetry) analysis is a thermal analysis technique used in the scientific field to study thermal transitions and thermal properties of materials.

This technique measures the differences in heat absorbed or released by a sample compared to a reference as it undergoes controlled heating or cooling cycles. DSC analysis is based on the principle that phase changes, transitions, or chemical reactions in a material involve the absorption or release of heat. During DSC, the sample and a reference sample, both subjected to the same temperature program, are heated or cooled.

The difference in heat between the sample and the reference is measured as a function of temperature or time. The sample and reference are placed in separate cells within a furnace. During the analysis, the furnace is heated or cooled according to a predefined temperature program. A temperature sensor detects the temperature of the samples, and a feedback system keeps the sample temperature constant relative to the reference. When the sample undergoes a thermal transition, such as a phase change (e.g., melting or crystallization), a chemical reaction, or a glass transition, there will be a heat flow associated with this transition. This heat flow causes a temperature difference between the sample and the reference, which is measured by the DSC. [25] [26]

2.1.6 Differential scanning calorimetry (DSC)

The membranes were analysed using differential scanning calorimetry (DSC) to evaluate their thermal stability. These analyses were carried out using a Netzsch DSC 204 F1 Phoenix differential scanning calorimeter (Figure 5). Heat flows were measured during heating and cooling cycles ranging from -65°C to 150°C at a rate of 10°C/min. The data obtained were processed using Netzsch Proteus analysis software.

Figure 5-Picture of DSC instrument

2.1.7 Microbalance

Gas permeation characteristic of the materials were evaluated using a surface measurement system, the Dynamic Vapor Sorption (DVS) Instrument (Figure 6). Through a series of several gas adsorption and desorption cycles on the membrane, the change in weight of the membrane was monitored. The cycles used varied from 0 to 80% of the partial pressure of the gas (CO_2 or N_2), and the maximum CO_2 absorption at each partial pressure value was calculated. The temperature was kept constant at 40°C in all experiments.

Figure 6-Picture of Microbalance

2.1.8 Microwave

Microwave reactors represent a revolutionary advancement in polymer synthesis. These reactors harness electromagnetic waves within a frequency range of 300 MHz to 300 GHz (Figure 7).

They facilitate rapid, uniform, and selective heating of reagents, expediting the chemical reactions vital for polymer formation. At the core of a microwave reactor lies the synthesis chamber, constructed from materials transparent to microwaves, such as quartz glass or specific polymers. This chamber is where the chemical magic happens. Inside, reagents are meticulously combined.

The process begins with the generation of microwaves, precisely controlled for frequency and power. These microwaves are then directed into the synthesis chamber, where they interact with the reagent molecules. This interaction induces a rapid surge in temperature, driving the chemical reaction forward at an accelerated pace. Throughout the process, sensors continuously monitor critical parameters, including temperature and pressure. [27]

This ensures that the reaction remains on track. Once the reaction reaches completion, the system can be efficiently cooled, effectively halting polymer synthesis. The benefits of microwave reactors in polymer synthesis are far-reaching. They significantly reduce synthesis times and energy consumption when compared to conventional methods. Moreover, they offer unparalleled control over reaction conditions, resulting in cleaner and more selective reactions with fewer unwanted byproducts.

These reactors find wide applicability, accommodating a diverse range of polymers and synthesis processes.

Figure 7-Picture of microwave reactor

2.1.9 Density

Density was evaluated by die-cut some specimens with a 1 cm diameter so that five cylinders were obtained. Of these, the mass (in mg) and thickness (in µm) were measured, and then the volume (thickness x area) was calculated.

2.2 Material

The following reagent and solvent were purchased from "Merk-Sigma-Aldrich":5,5′,6,6′-tetrahydroxy-3,3,3′,3′-tetramethyl-1,1′ spirobisindane; Dimethylformamide (DMF); Potassium bicarbonate ;

Sodium hydroxide; ethanol; methanol; o-Phenylenediamine; Eaton's reagent; Dimethyl sulfoxide (DMSO); m-cresol.

The monomer, 2,3,5,6- Tetrafluoroterephtanonitrile, was purchased from "Fluoro Chem".

2.3 Methods

2.3.1 Synthesis of PIM1

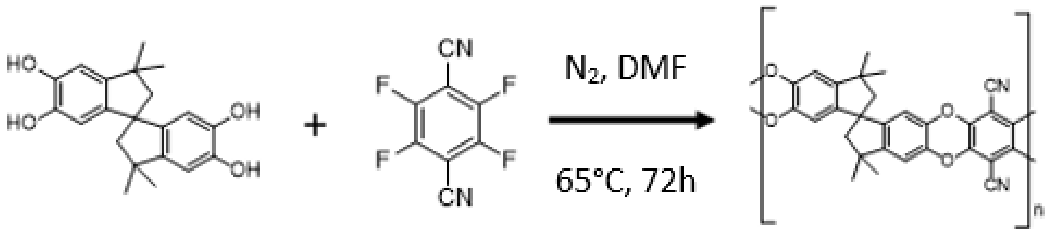

Figure 8- Schematic reaction of the PIM1 synthesis

The polymer was synthesized following the methods reported in the following articles from Budd at all. [28] A mixture of anhydrous K_2CO_3 (5.53g, 0.04mol, FW=138.205 g/mol), 5,5′,6,6′-tetrahydroxy-3,3,3′,3′-tetramethyl-1,1′-spirobisindane (3g, 0.008813mol, FW=340.41 g/mol), and 2,3,5,6-Tetrafluoroterephthalonitrile (1.76g, 0.008813mol, FW=200.096 g/mol) in dried DMF (60mL) was stirred at 65°C for 72 hours under a nitrogen atmosphere (Figure 8). After the reaction, the crude product was poured into 400 mL of water, and the precipitated solid was centrifuged twice with water and seven times with methanol to remove any acid residues. Finally, the product was placed in a vacuum oven at a temperature of 40°C for 24 hours, a fluorescent yellow solid was obtained as the pure product.

2.3.2 Synthesis of cPIM-1

Figure 9- Schematic reaction of the cPIM-1 synthesis

According to the literature [29], the synthesis of cPIM-1 is based on the concept of hydrolysing the nitrile group in PIM-1. As cited, PIM-1 powder is dissolved in a 20 wt% NaOH solution of a mixture of water and ethanol in a 1:1 ratio. The reaction was carried out using a microwave reactor at a temperature of 120°C, at a maximum pressure of 20 bar, for 1 hour, and at an agitation speed of 600 rpm (Figure 9). Upon completion of the reaction, due to the highly basic environment, a beaker containing the final product was prepared. An aliquot of HCl (37%) was added to the beaker to carefully adjust the pH of the solution, aiming for a range between 4 and 5. Subsequently, the product underwent filtration and was washed with water and methanol to remove any acid residues. Finally, the product was first placed in a vacuum oven at a temperature of 40°C for 24 hours and then in another vacuum oven at 100°C.

2.3.3 Synthesis of Benzimidazol-PIM

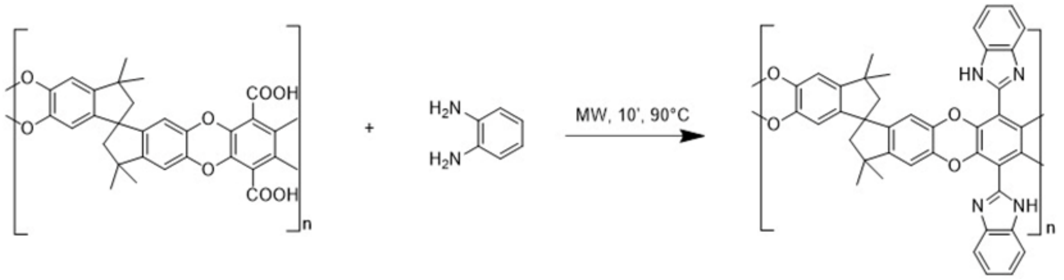

Figure 10- Schematic reaction of the Benzimidazol-PIM synthesis

The synthesis of Benzimidazole-PIM was carried out following the method proposed in the cited journal article from Olvera-Mancilla and others, which outlines the synthesis of polybenzimidazole (PBI). [17] Initially, 3 grams of cPIM-1 were mixed with 32.22 mL of Eaton's reagent for about 10 minutes, followed by the addition of 1.2 grams of 1,2-phenylenediamine. The reaction took place in a microwave reactor at a temperature of 90°C for a duration of 10 minutes, using a power of 100W (Figure 10). At the end of the reaction, the crude product is highly acidic due to the presence of methane sulfonic acid in the Eaton reagent, which imparts this strongly acidic characteristic to the final compound. For this reason, the crude was poured in a solution of water and potassium bicarbonate until the pH of the solution is neutral. Subsequently, the solution was left stirring for two hours and then subjected to filtration with water and centrifugation with methanol. Finally, the product was dried and placed in a vacuum oven at a temperature of 40°C for 24 hours and then in another vacuum oven at 100°C, to obtain the desired final compound, Benzimidazole-PIM.

2.3.4 Membrane preparation procedure

Initially, various solubility tests are carried out in different solvents. Once the solvent is found to be compatible and more soluble with the product, the process is optimized. Benzimidazol-PIM is soluble in DMSO and cresol. Finally, the membrane is spread by solvent casting following several steps:

1- dissolve the product in the solvent.
2- Pour the mixture on a support (petri dish) outlining the desired shape.
3- Evaporating the solvent.

After evaporation of the solvent, the membrane will detach from the support. Finally, it is placed in a vacuum oven at 40 ºC for 12h.

3 The synthesis of polymers

3.1 PIM1

This section describes the synthesis phases of the polymer PIM1 with their respective analyses and characterizations.

3.1.1 Synthesis of PIM1

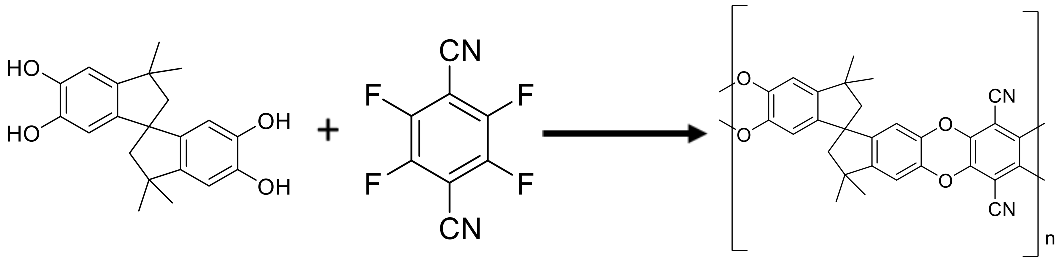

Figure 11- Schematic reaction of the PIM1 synthesis

The synthesis of PIM-1 starts with the 5,5′,6,6′-tetrahydroxy-3,3,3′,3′-tetramethyl-1,1′-spirobisindane (SPIRO) and tetrafluoroterephthalonitrile (TFTCN), which have ideal chemical properties for obtaining a high molecular weight reaction polymer (Figure 11). The reaction is an aromatic nucleophilic substitution consisting of a nucleophilic reagent capable of donating its electrons to an electrophilic species. TFTCN contains two cyanide groups, which weaken the C-F bond, making fluorine an excellent leaving group. The environment is turned basic by potassium bicarbonate ($KHCO_3$) that helps to deprotonate the hydrogen of the SPIRO hydroxyl group, facilitating nucleophilic attack and increasing the reaction's efficiency. It also helps to prevent the formation of an undesired byproduct like hydrofluoric acid (KF), producing potassium fluoride (KF) as precipitate instead. SPIRO, that contains hydroxyl groups, acts as nucleophiles mainly due to the negative charge on oxygen by deprotonation. The solvent used in the reaction is dimethylformamide (DMF) that improves the miscibility of the reagents, allowing them to interact effectively. [30] [31]

An inert environment by performing vacuum and nitrogen cycles both in the solutions and in the reactor is important, as oxygen in the air could oxidize the just formed polymer producing undesired reticulation.

The reactor is a three-necked flask purged with an inert gas and immersed in a bath of silicone oil at a temperature of approximately 65°C filled with potassium bicarbonate and DMF. The central neck of the flask is connected to a condenser to allow vapours to condense and return to the reaction volume.

The reagents are introduced after being dissolved in DMF and placed in an inert environment with vacuum-nitrogen cycles introduced into the reactor. Once the desired temperature is reached, following a 72-hour duration, a precipitate with yellowish-green hue emerges. (Figure 12)

Figure 12- Apparatus used for the synthesis of PIM1

The reaction is quenched in water, and the precipitate is subsequently cleansed through multiple washes using methanol followed by several rounds of centrifugation. (Figure 13)

Figure 13-Raw product at the end of the 72h reaction

Water helps not only to collect all the product obtained as it is not soluble in it, but it also helps in removing the salts produced in the reaction; while methanol is useful for removing unreacted organic molecules, by-products, and the organic solvent used (DMF).
At the end of the cycle, a solution consisting of the product at the bottom and a liquid phase containing excess water and substances is obtained, which is separated. In total, 4 cycles with water and 5 with methanol are performed. Finally, the product is placed in a vacuum oven at 40°C overnight and then in a Buchi oven at 100°C under vacuum until constant weight, ensuring the removal of all the solvents used so far to obtain a pure compound. (Figure 14)

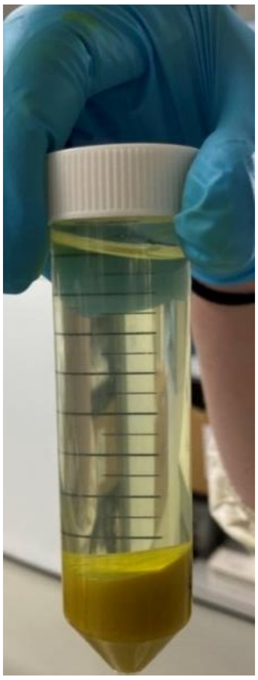
(a)

(b)


Figure 14- a) picture of Falcon with methanol after centrifugation. b) the final dry product.

3.1.2 Characterizations of PIM1

Even if it is an established protocol, it is imperative to confirm the identity of the obtained products PIM1. To validate this assertion, it is essential to conduct an array of analysis, including ATR analysis, TGA, TGA-IR, and DSC.

3.1.2.1 ATR analysis of PIM1

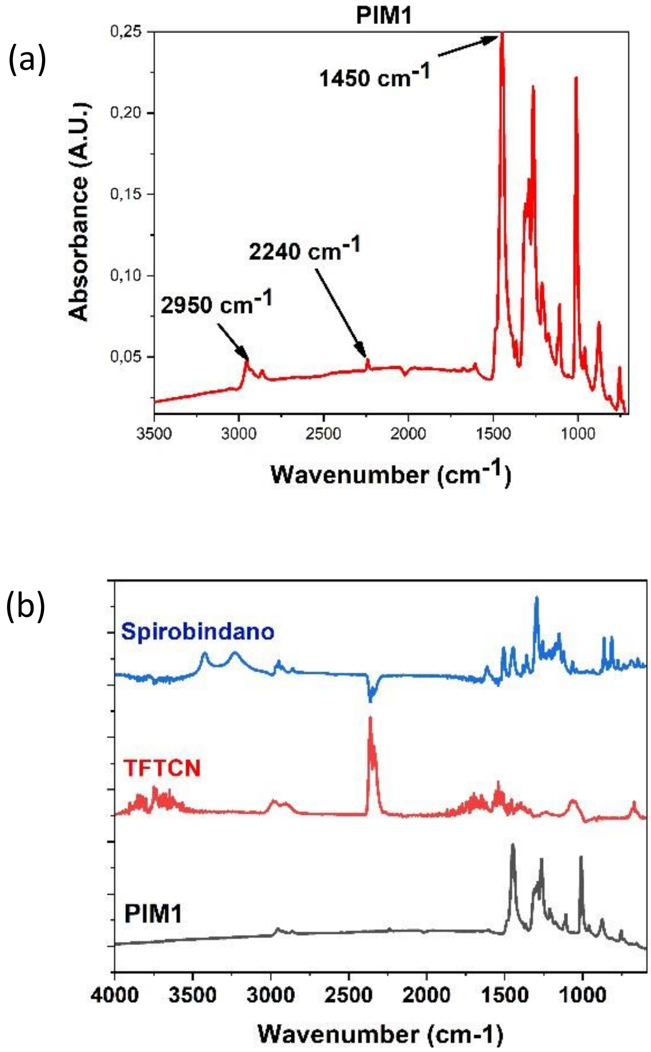

Figure 15-ATR analysis of a) PIM-1 b) comparison between PIM1 (black), TFTCN (red) and SPIRO (blue).

In Figure 15a the PIM1 ATR spectra is presented, and it can be noted that the stretching of SPIRO at 3200 cm^{-1} and 3400 cm^{-1} related to O-H bonds are absent in PIM1. (Figure 15b)

Also, the signals between 1000 and 1400 cm^{-1} related to the stretching of the C-F bond present in the TFTCN reagent are absent in the PIM-1 spectrum. The presence of C-H bonds with sp^3 hybridization and C=H bonds with sp^2 hybridization is highlighted by signals around 2950 cm^{-1}. There are also signals of the bending of the -OH bond corresponding to the peak at 1450 cm^{-1}. [32]

Lastly, the signal of the -CN bond, characteristic of PIM1, is well defined at 2240 cm^{-1}, which is shared with the TFTCN reagent. [33] [39]

3.1.2.2 TGA-IR analysis of PIM1

(a)

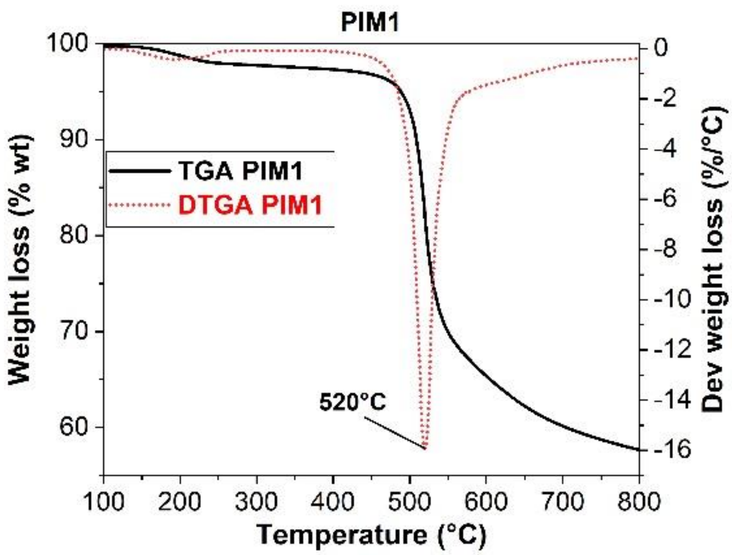

(b)

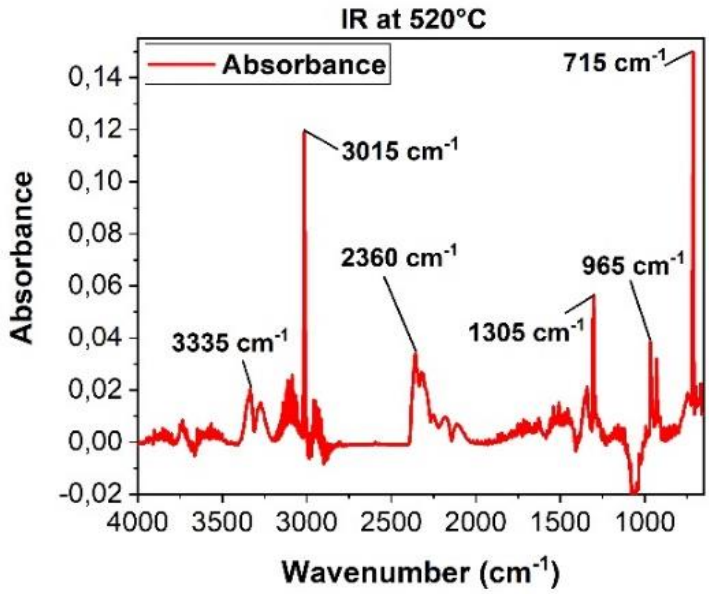

Figure 16- a) TGA analysis of PIM-1 b) IR spectrum related to weight loss at 520°C

From the observation of the spectra related to the thermogravimetric analysis (Figure 16 a), a small weight loss at 200°C, corresponding to the loss of small molecule presented in the PIM1 micropore is observed. However, as confirmed in the scientific article from at all [34], the polymer exhibits remarkable thermal stability, with its thermal degradation displaying a peak degradation point at 520°C (Figure 16 b), beyond which there is a swift decomposition resulting in the loss of 40% of the initial product by weight [29]. The gad produced in this degradation step is analysed by IR. The spectrum at 520°C attributed to the degradation of the organic matrix of PIM-1, contains the characteristic signals of the small molecules generated such as:

- at 3015 cm^{-1} and 715 cm^{-1}, stretching related to the methane molecule.
- at 965 and 3335 cm^{-1}, stretching and banding related to the NH_3 molecule.
- at 2360 cm^{-1}, related to the $-CO_2$ groups.

- at 1305 cm^{-1}, related to the stretching of the C-O bond.

3.1.2.3 DSC analysis of PIM1

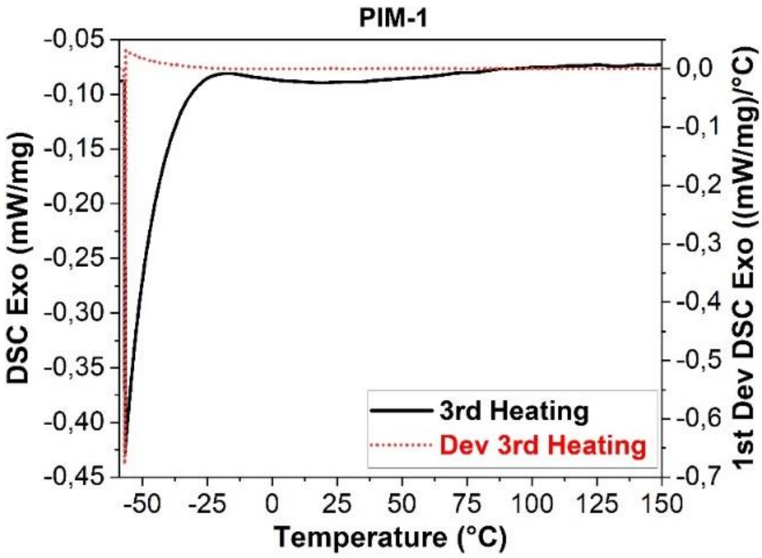

Figure 17-DSC spectrum relating to the analysis of PIM-1

In this analysis, Figure 17, the sample underwent numerous cycles of heating and cooling to evaluate its thermal characteristics. The initial cycles were excluded from consideration as their primary objective was to establish the sample's thermal history. Consequently, upon analysing the last heating cycle and its derivative, it can be confidently concluded that the polymer does not manifest any discernible thermal transitions, consistent with expectations.

3.2 cPIM-1

This section describes the synthesis phases of the polymer cPIM-1 with their respective analyses and characterizations.

3.2.1 Synthesis of cPIM-1

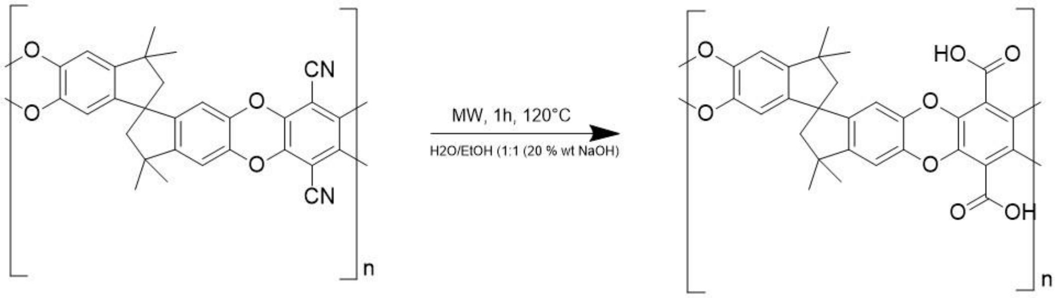

Figure 18- Schematic reaction of the cPIM-1 synthesis

The cPIM-1 is produced by the PIM1 nitrile group hydrolysis in a solution of 20% by weight of NaOH in water and ethanol in a 1:1 weight ratio, The addition of soda with water is a step that requires caution due to the highly exothermic reaction. (Figure 18)

The sodium hydroxide plays a fundamental role in the context of this reaction, as it provides an extremely basic environment, facilitating the hydrolysis of the -CN groups in PIM1 to $-COO^{-}Na^{+}$ groups. To produce the carboxylic acid, it is necessary to acidify the solution by using hydrochloric acid.

Hydrochloric acid addition also allows the formation of NaCl by-product, that is easy to handle due to its solubility in an aqueous environment.

The cPIM-1 was prepared by adding PIM1 with ratio of 1:16 mass/volume. The reaction was conducted using a microwave reactor, which offers significant advantages, including homogeneous heating resulting from heat flow radially, from the centre of the molecule outward. Furthermore, this approach allows for optimal thermodynamic control of the reaction, as it is possible to precisely regulate power, exposure time, pressure, and temperature.

This approach also allows operation at temperatures higher than the boiling points of the solvents, and a pressure up to 20 bar in order to improve significantly the reaction kinetics. Specifically, the reactor is set at a temperature of 120°C for 1 hour, with a rotation speed of 600 rpm, surpassing the boiling points of water (100°C) and ethanol (78°C). This optimal configuration ensures an efficient and controlled reaction process, guaranteeing accurate and consistent results.

At the end of the reactive process in the microwave reactor, a gel-like product is obtained. (Figure 19)

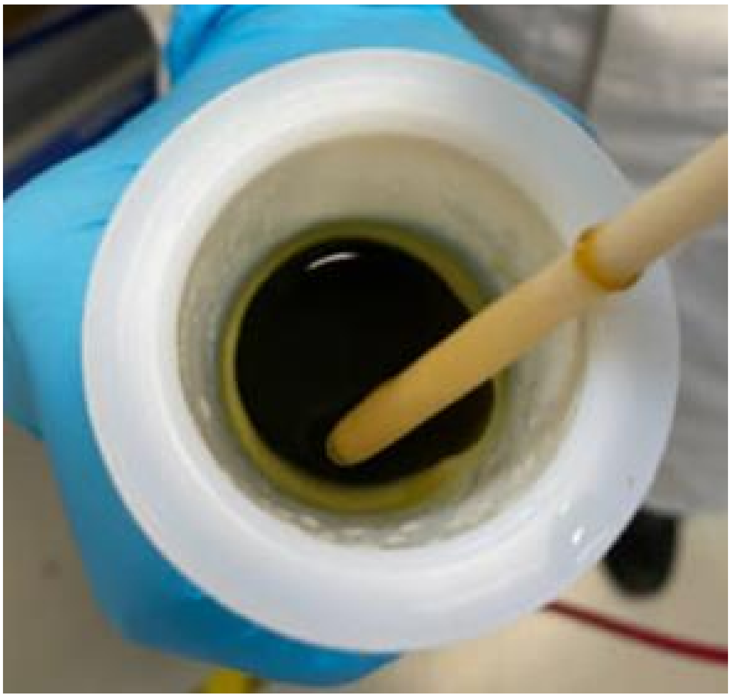

Figure 19-Fluid inside the reactor

This gel is transferred to a stirred flask containing water, and hydrochloric acid (37% molar) is added until an acidic pH in the range of 4 to 5 is reached. (Figure 20)

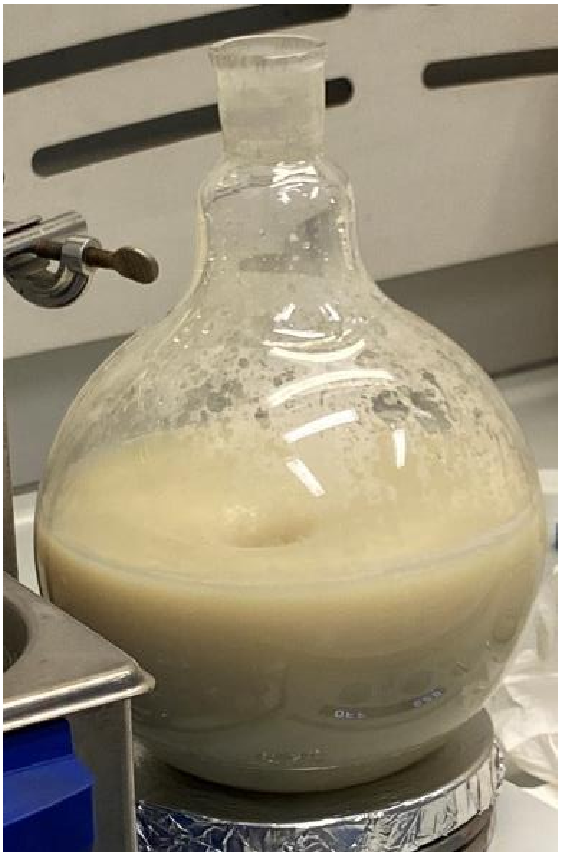

Figure 20-Flask containing the raw product at the end of the reaction dissolved with water and hydrochloric acid.

Subsequently, a vacuum filtration of the solution was performed using water initially to remove the acidic component of the solution and the sodium chloride (NaCl) generated as a byproduct of the reaction.

Subsequently, methanol filtration is employed, as it has demonstrated exceptional efficacy in purging undesirable molecules, including byproducts and unreacted reagents. (Figure 21)

The methanol was chosen as washing solvent due to its high evaporation rate that allows a faster drying.

Figure 21-Filtering system between methanol and cPIM-1

The filtrate was subsequently dried under vacuum process in an oven at 40°C for one day, and then placed in a vacuum system at 100°Cuntil constant weight. The choice to adopt a progressive vacuum and use a perforated aluminium foil cap is due to the possible presence of solvent (ethanol) trapped in the pores of the cPIM-1 polymer, which could evaporate rapidly and cause slight internal pressures, posing a risk to the stability of the compound and potentially leading to minor explosions.

3.2.2 Characterizations of cPIM-1

Even if it is an established protocol, it is imperative to confirm the identity of the obtained products cPIM-1. To validate this assertion, it is essential to conduct an array of analysis, including ATR analysis, TGA, TGA-IR, and DSC.

3.2.2.1 ATR analysis cPIM1

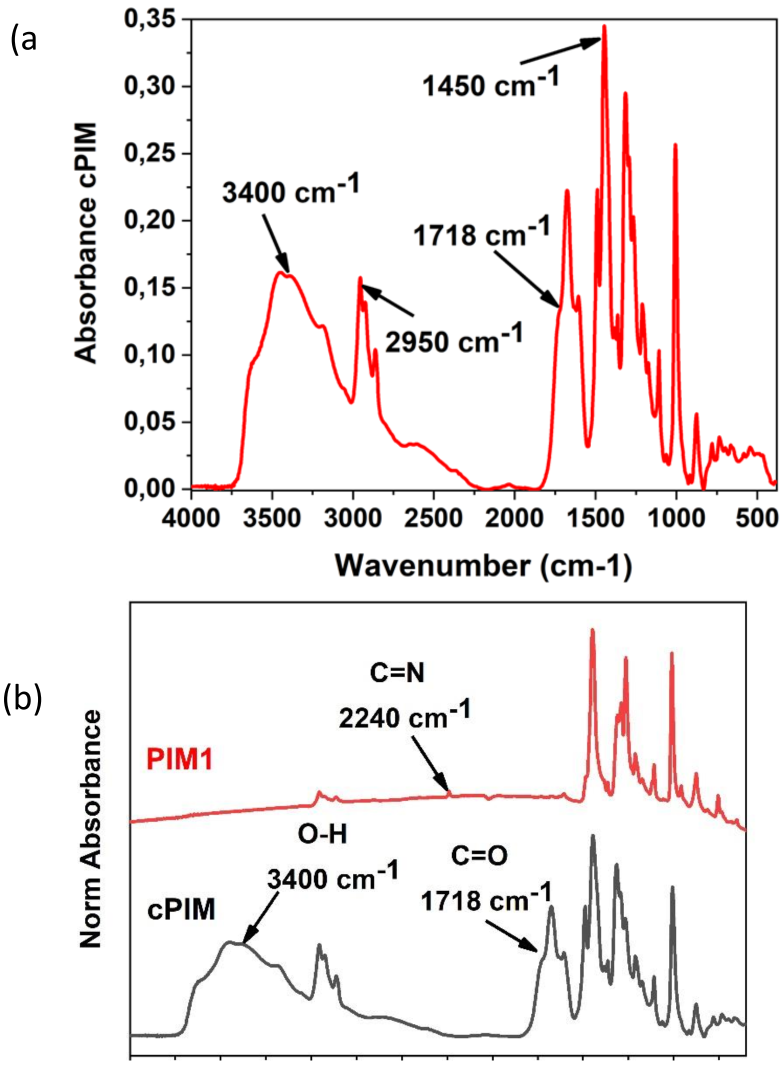

Figure 22-ATR analysis of a) cPIM-1 and b) comparison between IR spectrum of PIM-1(red) and cPIM(black).

ATR analyses of the resulting polymer (Figure 21) shows the characteristic signals indicating the formation of the carboxylic group and the complete absence of the -CN group present in the initial polymer can be observed. (Figure 22 a,b)

These results are also supported by the article [29], where the presence of signals at 1718 cm^{-1} (corresponding to C=O stretching) and around 3400 cm^{-1} (corresponding to the O-H bond of the hydroxyl group) supports the formation of the carboxylic group, while the absence of the -CN signal at 1260 cm^{-1} confirms the elimination of the cyanide group. Signals related to the stretching and banding of C-H bond at 1450 cm^{-1} and 2950 cm^{-1} are also present.

3.2.2.2 TGA-IR analysis cpim1

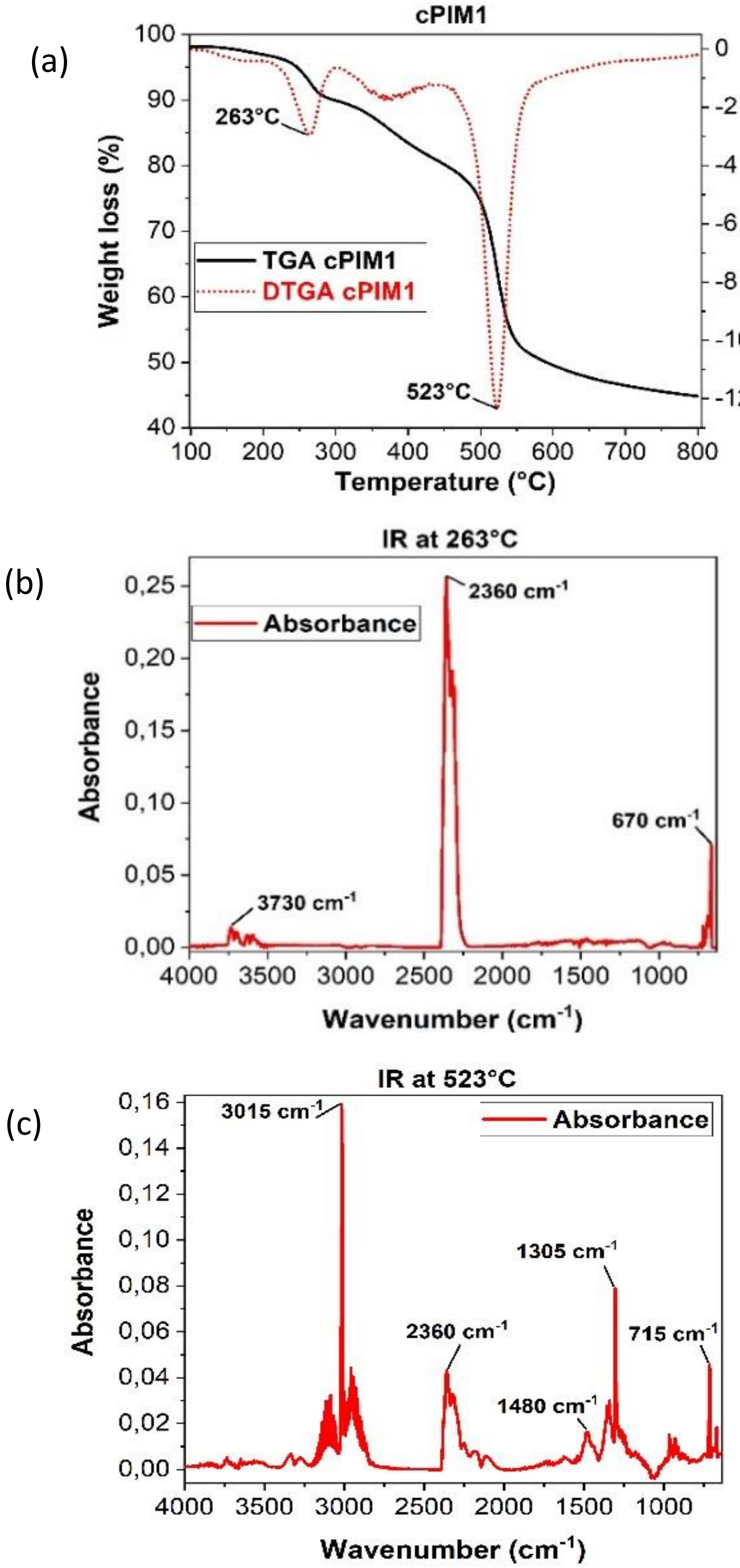

Figure 23-a) TGA analysis of cPIM-1 b) IR spectra relating to the weight losses at 263°C c) IR spectra relating to the weight losses at 523°C

The analysis conducted aimed to investigate the thermal properties of the polymer in question. (Figure 23 a)

From the obtained thermogravimetric curve, a clear double weight loss is evident at 263°C and 523°C. To determine the nature of these weight losses, an infrared analysis of the gases released during the sample's decomposition was carried out. This approach allows for the identification of the involved chemical species and understanding the nature of the thermal transformations that occurred during the decomposition process. The first spectrum obtained, Figure 23 b, at 2360 cm^{-1}, corresponds precisely to the signal of carbon dioxide formed by the decarboxylation of the hydroxyl group. [35] At 715 cm^{-1} and 3015 cm^{-1} a stretching signals of methane molecule is observed. Subsequently, a pronounced weight loss is evident around 520°C, Figure 23 c, like what was observed in the analysis of PIM-1, and this phenomenon is accompanied by an infrared spectrum that precisely identifies the series of signals related to the polymer's core.

3.2.2.3 DSC analysis cPIM1

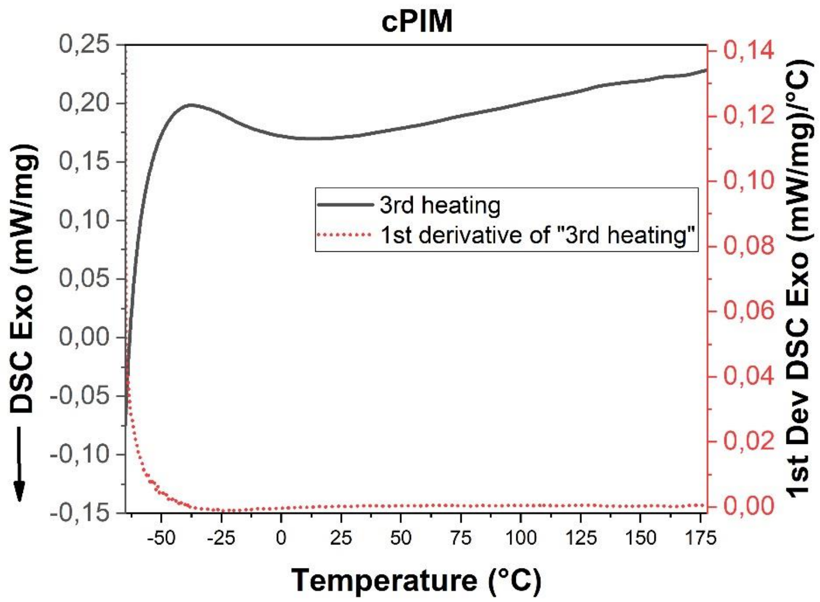

Figure 24-Related spectrum of DSC analysis of cPIM-1

In this analysis, the sample underwent numerous cycles of heating and cooling to evaluate its thermal characteristics.

The initial cycles were excluded from consideration as their primary objective was to establish the sample's thermal history. Consequently, upon analysing the last heating cycle and its derivative, it can be confidently concluded that the polymer does not manifest any discernible thermal transitions, consistent with expectations. (Figure 24)

3.3 Benzimidazol-PIM

This section describes the synthesis phases of the polymer PIM1 with their respective analyses and characterizations.

3.3.1 Synthesis of Benzimidazol-PIM

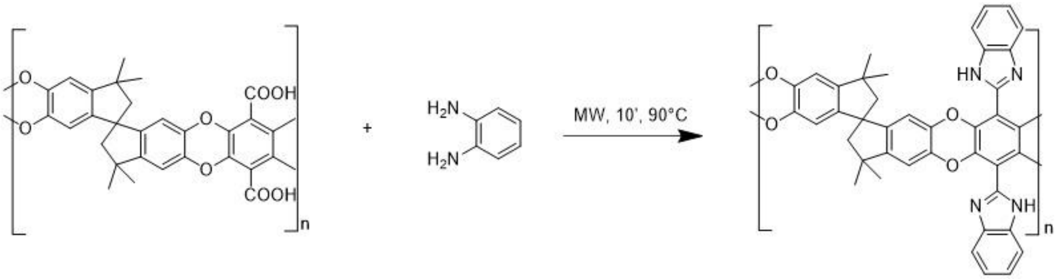

Figure 25- Schematic reaction of the Benzimidazol-PIM synthesis

The synthesis of this new polymer requires the implementation of a reaction aimed at replacing the carboxylic groups present in cPIM-1 with the benzimidazole functional group. (Figure 25)
As documented in the cited article from Olvera-Mancilla and others [17], the optimal quantities of each reagent have been calculated, considering the double substitution of the hydroxyl group in each monomer of cPIM-1. This approach was adopted to ensure the achievement of the desired molecular structure in the resulting polymer and to maximize the efficiency of the reaction.

Table 1- Amount of reagent for the synthesis of Benzimidazol-PIM

Reagent	cPIM	Fenilendiammina	Eaton's Reagent
Quantity	3 g	0.011 mol	32.22 ml

Two syntheses of this polymer were carried out, in which the order and timing of reagent addition were modified. Initially, a synthesis of the cPIM-1 polymer was conducted, followed by the sequential addition of phenylenediamine and, finally, the Eaton reagent. However, this procedure resulted in the formation of a rather granular and difficult-to-solubilize final product. To improve the synthesis process, it was hypothesized to reverse the order of reagent addition, introducing the Eaton reagent first and then the phenylenediamine.

This choice was guided by theoretical considerations, as in an acidic environment, the polymer tends to encourage the protonation of the -C=O group in the carboxylic group, thereby facilitating better amine substitution. Conversely, as occurred in the first synthesis, an acidic environment protonates amines, reducing their nucleophilic characteristics and consequently decreasing the overall efficiency of the reaction. Therefore, the strategy of reversing the order of reagent addition was adopted to optimize the polymer synthesis and maximize the yield of the final product, considering the theoretical considerations regarding the influence of the acidic environment on amine substitution reactions.

To conduct the synthesis, the acidic solution of the Eaton reagent, in predetermined quantities, and the calculated amount of polymer were introduced into the reactor. The mixture was left stirring for approximately 30 minutes, during which a rapid change in the colour of the solution was observed, transitioning from green to intense red. Subsequently, phenylenediamine was added to the system, resulting in a homogeneous compound ready to undergo the reaction.

As mentioned in the reference article [36], the reaction takes place in a microwave reactor operating at a temperature of 90°C and 20 bar,

Figure 26-Raw product at the end of the reaction in the microwave

with a power of 100W, for 10 minutes. At the end of the reaction, a solid plug was obtained, below which a reaction product with a liquid-pasty consistency and dark red colour was formed. (Figure 26)

Due to the acidic nature of the reaction product, it was necessary to quench the reaction by addition to an aqueous solution of potassium bicarbonate. This procedure not only helped quench the acidity but also facilitated the precipitation of amines, increasing the product yield as the amines transitioned from the $NH4^+$ form to the NH_3 form in the organic phase.

The addition of potassium bicarbonate to the solution generated foam, which can be identified as CO_2 released during the neutralization process. Subsequently, after 2 hours of stirring to allow for the precipitation of the product, a double filtration process was carried out, first under vacuum using water, and then by centrifuging the filtrate with methanol.

The resulting solid was placed in a vacuum oven at 40°C and left overnight before being transferred to the vacuum oven at 100°C for an additional night.

Figure 27-Dusty form of Benzimidazol-PIM

The result obtained is a powdery solid compound with a yield of 83%. (Figure 27)

3.3.2 Characterization of Benzimidazol-PIM

Even if it is an established protocol, it is imperative to confirm the identity of the obtained products cPIM-1. To validate this assertion, it is essential to conduct an array of analysis, including ATR analysis, TGA, TGA-IR, and DSC.

3.3.2.1 ATR analysis of Benzimidazol-PIM

(a)

(b)

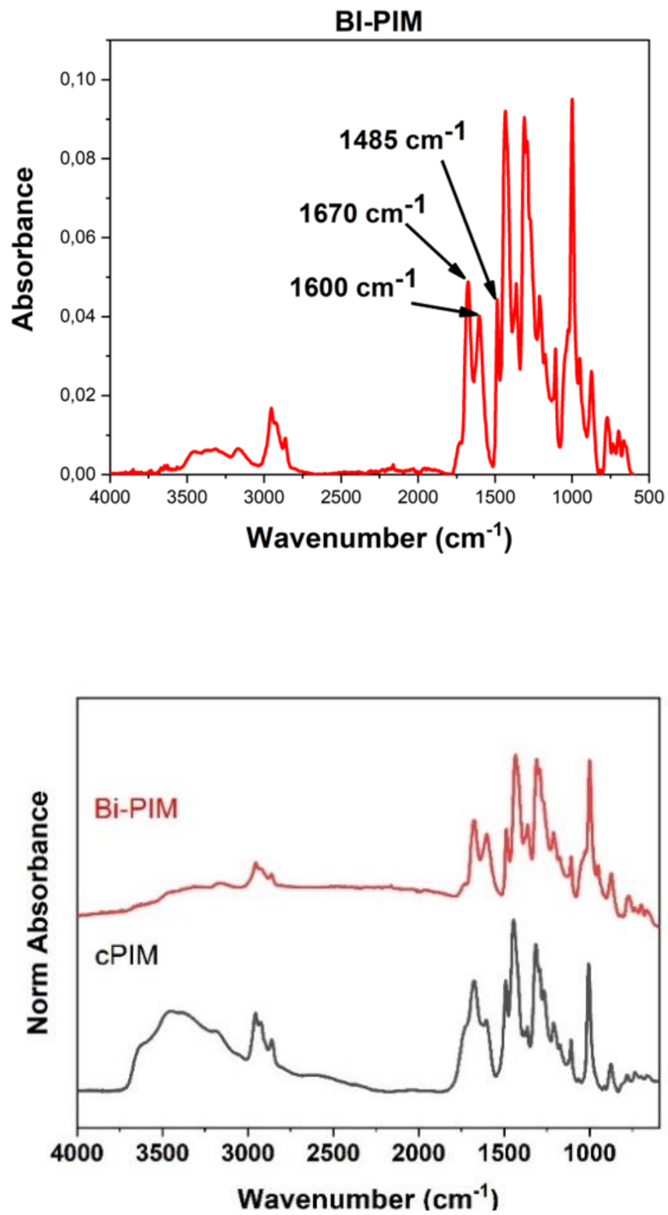

Figure 28-a) ATR spectrum of Benzimidazol-PIM b) comparison between cPIM-1 (black) spectrum and Bi-PIM (red) spectrum.

From ATR analyses (Figure 28 a,b) of product, it is possible to notice the total absence of the broadband at 3400 cm^{-1} and the peak at 1718 cm^{-1}, both related to the carboxylic group.

At the same time, the appearance of new signals at 1485 cm^{-1} and around 1600 cm^{-1} corresponding to the vibrations and deformations of the benzimidazole ring is observed, a result also confirmed in the literature from Mallakpour at all. [37] [38]

The synthesis of the new Benzimidazol-PIM polymer is successfully confirmed through the observation of the remaining peaks, which exactly correspond to the core of the polymer, highlighting the same characteristic signals present in both cPIM-1 and PIM-1 as shown in Figure 26 b.

3.3.2.2 TGA-IR analysis of Benzimidazol-PIM

(a)

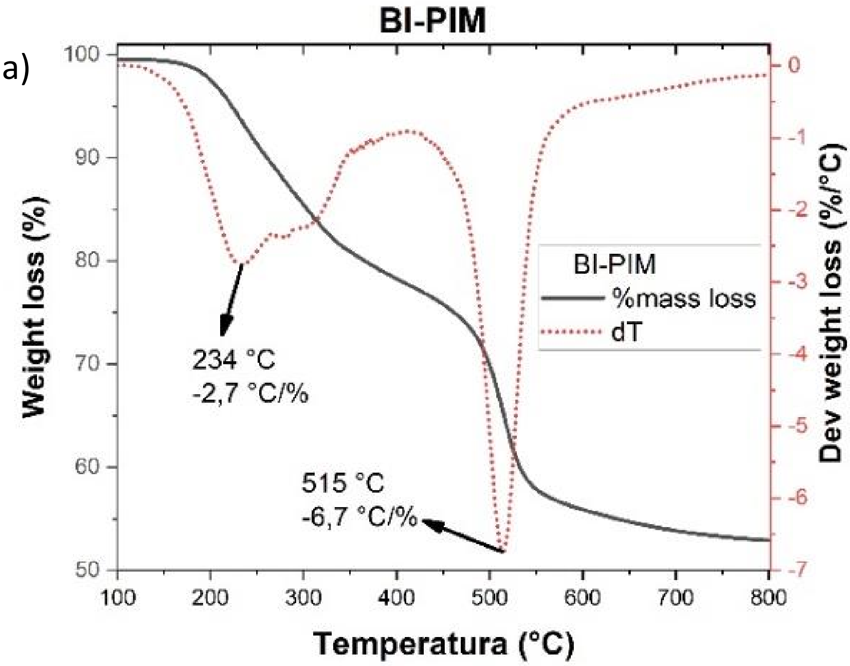

(b)

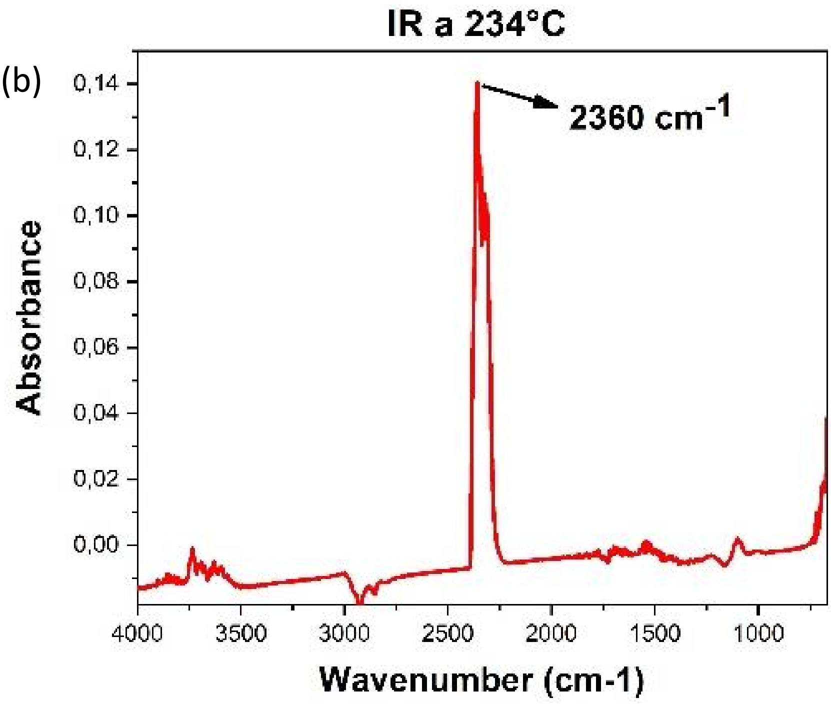

(c)

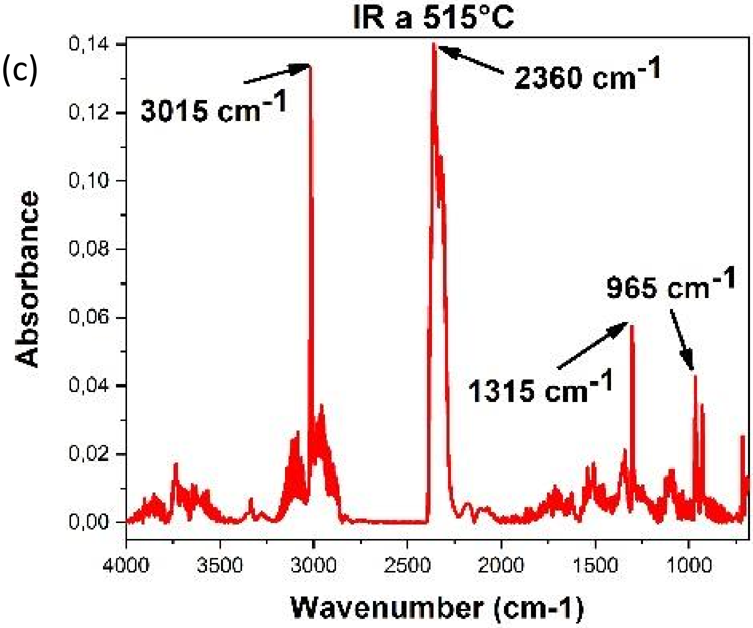

Figure 29-a) TGA spectrum of Benzimidazol-PIM b) IR spectra relate to degradation observed at 234°C. c) IR spectra relate to degradation observed at 515°C.

The thermogravimetric analysis of the polymer reveals a double weight loss: the first loss occurs at 234°C, resulting in about a 20% reduction in the sample's weight, while a second degradation occurs at 515°C. (Figure 29 a)

The analysis of the infrared spectra related to the first degradation highlights the presence of a peak at 2360 cm^{-1}, indicative of the formation of CO_2. (Figure 29b)

In the second spectrum, Figure 29 c, signals at 3015 cm^{-1} and 715 cm^{-1} are related to the stretching of methane molecule; at 1315 cm^{-1} there is the stretching of C-O bond and at 965 cm^{-1} and around 3330 cm^{-1} are related to the stretching of $-NH_3$ molecule. This signals are clearly detectable due to they are present in both PIM1 and cPIM-1 polymers. These results confirm the similarity between the new Benzimidazol-PIM polymer and cPIM-1, reinforcing the evidence of the successful synthesis of Benzimidazol-PIM and confirming the identity of the structural characteristics of the obtained material.

3.3.2.3 DSC analysis of Benzimidazol-PIM

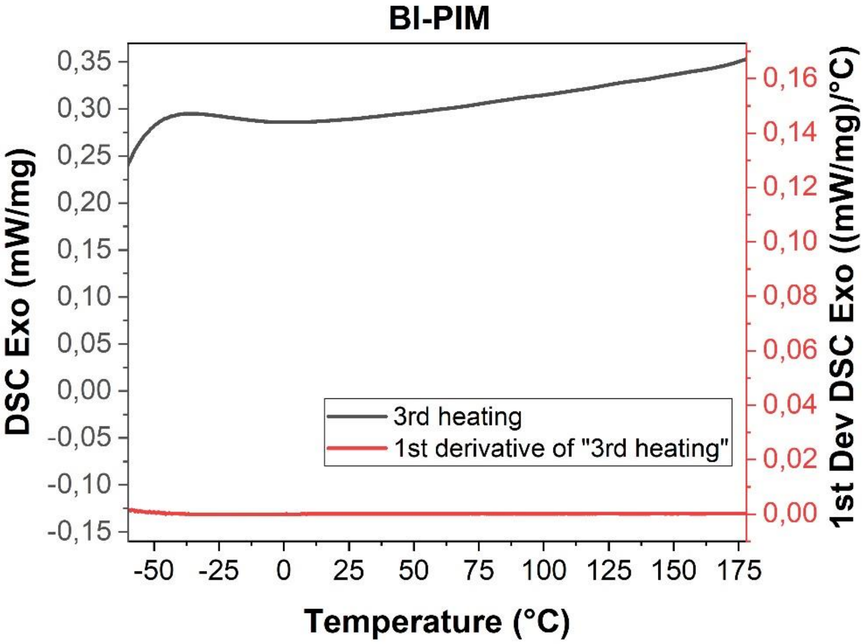

Figure 30-Spectrum related to the DSC analysis of Benzimidazol-PIM

In this analysis, the sample underwent numerous cycles of heating and cooling to evaluate its thermal characteristics. The initial cycles were excluded from consideration as their primary objective was to establish the sample's thermal history. Consequently, upon analysing the last heating cycle and its derivative, it can be confidently concluded that the polymer does not manifest any discernible thermal transitions, consistent with expectations. (Figure 30)

3.3.3 Solubility tests of Benzimidazol-PIM

To determine the solubility of the Benzimidazol-PIM polymer, solubility tests were conducted using various solvents.

8 ml vials containing a sample of Benzimidazol-PIM (25 mg) and an appropriate amount of solvent were used. The solvents selected for the tests were chosen based on their properties and in accordance with literature [4]. The tested solvents included chloroform, tetrahydrofuran [THF] (both advantageous due to their low boiling points allowing for evaporation at room temperature), N-Methyl-2-pyrrolidone (NMP), Dimethylformamide (DMF), Dimethyl Sulfoxide (DMSO), acetic acid, hydrochloric acid (HCl), phosphoric acid, and cresol.

From the analysis of the results, it was observed that only a few solvents were capable of partially dissolving the Benzimidazol-PIM product. The only solvents that showed solubilization capacity were NMP and DMSO (3.5 ml each), which were sonicated and heated on a hot plate to 150°C, as both are high-boiling solvents. Furthermore, it was found that cresol (1.5 ml) could optimally dissolve the polymer. Based on the conducted analyses, it was highlighted that the polymer is insoluble when individually tested in various solvents.

Consequently, a solvent combination was evaluated with the aim of solubilizing the polymer. The optimal combination was identified using a mixture of DMSO and cresol. This specific solvent combination successfully demonstrated the capacity to solubilize the Benzimidazol-PIM polymer, making it suitable for solvent-casting experiments.

This information will be valuable in determining the optimal method for processing the polymer and preparing membranes necessary for further studies and applications.

THF	No
H2O	No
$CHCl_3$	No
DMF	Dispersion up to 4ml
NMP	Dispersion up to 4ml
DMSO	Dispersion up to 4ml
MeOH	No
Cresol	Dispersion up to 4ml
Acetic acid	No
HCl	No

Table 2- Solubility tests with different solvents.

3.3.4 Solvent casting

To obtain the membranes, it's necessary to create a well-dissolved solution with the polymer within it. In this regard, a vial was prepared by adding approximately 50 mg of Benzimidazol-PIM with 0.014 mol of DMSO (a high-boiling solvent) and 0.2/ 0.3 ml of cresol (a high-boiling solvent capable of dissolving the polymer). The solution was agitated and heated in an oil bath at 130°C until a homogeneous solution was achieved.

Subsequently, the solution was spread using a pipette to evenly distribute the compound on a plate set at 120°C. (Figure 31) This process creates a liquid layer that, over time, allows for slow and controlled evaporation of the solvents, thereby obtaining the desired membrane. (Figure 32)

Figure 31-Spreading of the solution on petri dishes.

Figure 33-Final membrane.

To assess the thickness and density of the membrane, samples were prepared by cutting into specific shapes and 1 cm diameter discs. (Figure 33)

Figure 32-Membrane lashes.

These samples will be placed in a vacuum oven (Buchi) at 100°C for one day to remove any residual solvent traces.

At the end of the process, the samples are weighed and analysed using specialized equipment, which is useful for measuring their thickness and, in turn, calculating the density of the product directly.

These analyses will accurately define the characteristics of the obtained membrane, contributing to an understanding of its physical properties and potential applications in the scientific and technological fields.

The obtained values have been processed in Excel, considering error propagation as well. Following this, the extracted data is tabulated.

Table 3- Characteristics of the membrane of Benzimidazol-PIM

Mass (g)	0.00255 ± 0.00031
Thickness (μm)	29.4 ± 6.24
Volume (cm^3)	0.00231 ±0.00063
Density (g/ cm^3)	1.124 ± 0.00066

Furthermore, the stamped samples are preheated at 80°C under vacuum for 10 hours to stabilize the membrane. Subsequently, the samples are analysed using a microbalance.

The microbalance is a highly sensitive instrument capable of assessing the weight difference of the stamped samples before and after gas permeation through the membrane. This method allows attributing gas absorption properties to the membrane.

Through this analysis, it will be possible to understand the membrane's gas absorption capabilities for specific gases, providing crucial information for evaluating the material's performance and potential applications in scientific and technological fields, such as selective gas separation or the absorption of specific substances.

3.3.5 Pure gas absorption measurements on membranes

Gas permeation characteristics of Benzimidazol-PIM membranes were included from studies performed outside this thesis, to show an example of gas permeability test for this membrane. In fact only CO_2 measures were reported while it should have been more useful because of the use planned for the membrane.

Namely permeability, diffusivity and solubility tests were performed using a Dynamic Vapor Sorption (DVS) instrument following the method previously described. [40]

Future work will be focused on testing other gases as N_2, O_2 and H_2.

3.3.5.1 Permeability

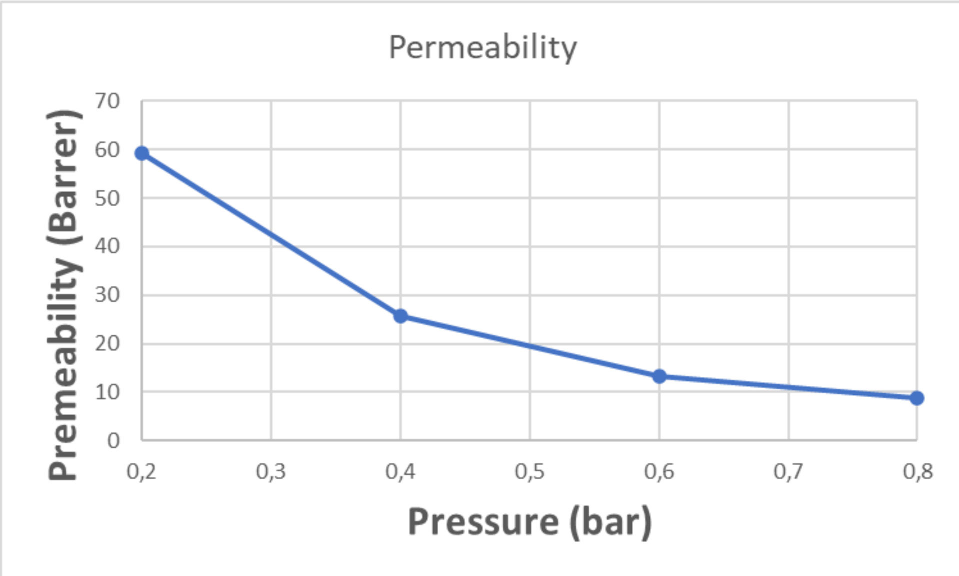

Figure 34-Permeability trend in pressure range of 0.2 and 0.8 bar

The permeability of a membrane is a measure of its ability to selectively allow specific gases to pass through it. It represents a key parameter for evaluating the effectiveness of membrane capability to separate and t concentrate the gases, such as in the purification or capture of CO_2.

Regarding membranes used in fuel cell or electrolyser applications, gases crossover through the membrane are an important factor to be consider. Here we are reporting only studies based on CO_2.

In the Figure 34, the permeability of the membrane to CO_2 is shown in a partial pressure ranging from 0.2 up to 0.8 bar. The observation of permeability decrement by increasing partial pressure is reasonably due to phenomena of molecular adsorption on the surface of the membrane.

This behaviour suggest that higher partial pressures promotes the adsorption of CO_2 molecules reducing the permeability.

This information provides a clear indication of how operative conditions can affect the membrane performance for both industrial or environmental applications.

3.3.5.2 Diffusivity

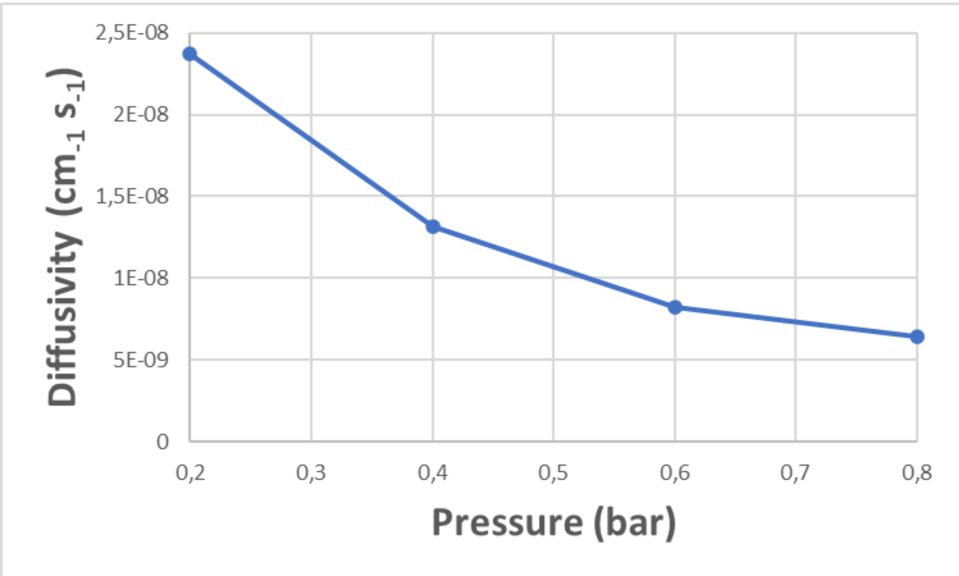

Figure 35-Diffusivity trend in pressure range of 0.2 and 0.8 bar

Diffusivity is a critical parameter in the study of membrane behaviour. Diffusivity value define the migration ability of through a material under a concentration gradient and differential pressure.

In figure 35, CO_2 diffusivity is evaluated in a partial pressure range from 0.2 up to 0.8 bar observing a clear decrement with the increment of partial pressure values. This is due to the denser packing of CO_2 molecules at higher pressures resulting in a mobility reduction.

3.3.5.3 Solubility

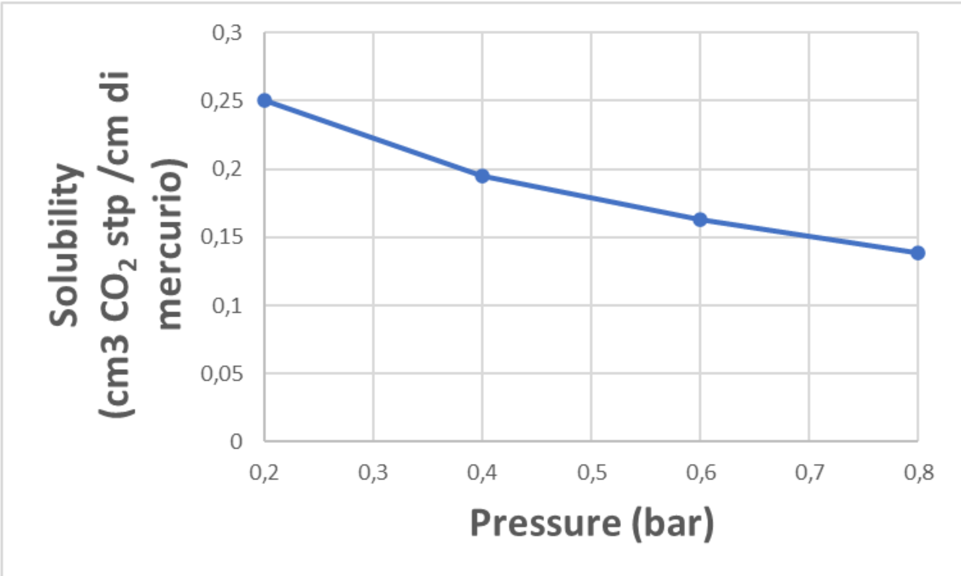

Figure 36-Solubility trend in pressure range of 0.2 and 0.8 bar

Solubility is a fundamental property that characterizes a substance's ability to dissolve in a given material under specific conditions of pressure and temperature.

Solubility plays a crucial role in processes like gas absorption or separation, where controlled interaction between the gas and the membrane is essential.

In Figure 36, Solubility is evaluated in a partial pressure range from 0.2 up to 0.8 bar observing a decrement by increasing the partial pressure values.

4 Conclusion

This thesis project constitutes a comprehensive study and development endeavour focused on an innovative proton exchange membrane designed to possess superior characteristics and properties compared the existing counterparts. Presently, the widely adopted membrane is Nafion, renowned for its impressive proton conductivity and high flexibility.

However, it is important to notice that Nafion, being a perfluorinated and sulfonated polymer, lacks an inherent proton-conducting medium, necessitating the presence of water for effective conduction. The reliance on water represents a limitation on its operational temperature, which should not exceed 90 degrees Celsius.

To address this, an intrinsically microporous polymer (PIM) was investigated, characterized by a chemical structure that endowed with excellent conductive attributes but reduced sensitivity to temperature fluctuations. The primary objective of this thesis was to substitute a functional group within the PIM monomer (-CN group) with a benzimidazole group. This decision was inspired by prior studies on polybenzimidazole, a polymer composed of benzimidazole chains renowned for their exceptional thermal and chemical stability, as well as outstanding corrosion resistance.

The development of this novel polymer involved the synthesis reaction of PIM1. Subsequently, cPIM-1, a polymer sharing the core structure of PIM1 but featuring a functional carboxyl group (-COOH) instead of the -CN group, was synthesized. Finally, the synthesis of Benzimidazole-PIM presented various challenges about factors like solubility, reaction duration, and operational conditions. Despite these challenges, a series of rigorous tests were conducted to refine the synthesis process for Benzimidazole-PIM, ultimately leading to an optimized protocol.

Subsequent stages involved comprehensive solvent compatibility tests and membrane production efforts. The membrane-laying process encountered several intricacies, but the obtained results affirm the effectiveness of the synthesis.

In summation, this thesis constitutes a substantial contribution in the field of polymeric material research and the development of sustainability-focused technologies. I appreciate the modest role played in this endeavour and eagerly anticipate witnessing how the undertaken work may positively impact the future of hydrogen-related technologies and polymeric materials.

---

5 Potential future application

The synthesis of the Benzimidazole-PIM membrane represents a tangible advancement towards its potential integration in the field of proton exchange membrane fuel cells and sustainable mobility.

In view of future perspectives, it is imperative to refine the polymer synthesis procedure, with a specific focus on achieving enhanced solubility and augmenting the mechanical properties of the membrane.

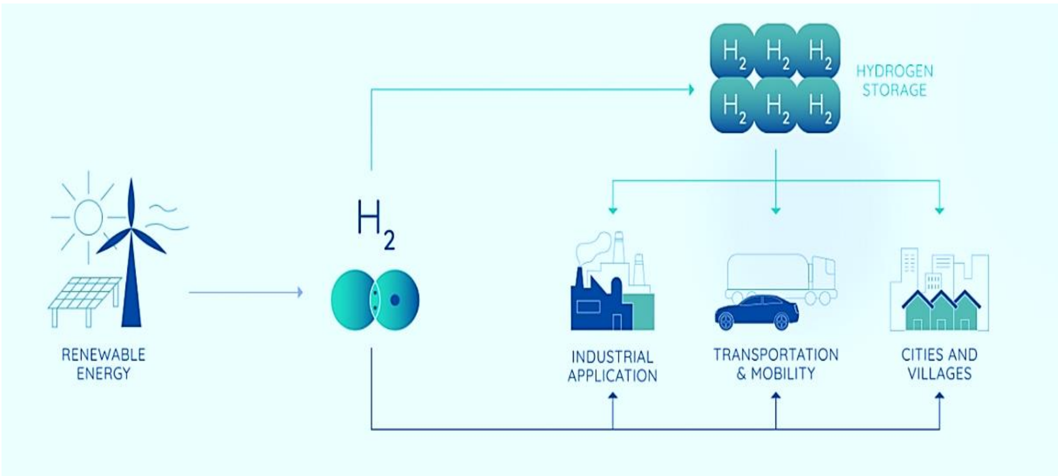

Figure 37-picture of renewable energy from H2

An approach highly recommended is to conduct experiments on doping with phosphoric acids and their derivatives to improve ionic conductivity, thereby ensuring more efficient ion transport. This strategy also aims to enhance the mechanical properties and thermal stability of the membrane. Considering more industrial applications within the context of transitioning towards renewable energy sources, as the industry endeavours to move away from fossil fuel-based energy in favour of renewable sources, new solutions are requisite to ensure comparable performance.

The adoption of a membrane that is both sustainable and high-performing in ionic conduction within fuel cells would lead to heightened efficiency in green energy production, reducing carbon footprint to zero and achieving high-quality hydrogen production, as asserted in the H2Future project. [41]

However, it is imperative to emphasize that further research and in-depth studies are required to refine its application and practical utility, thus ensuring the full realization of its extraordinary potential.

6 References

[1] Johnston, B., Mayo, M. C., & Khare, A. (2005). Hydrogen: the energy source for the 21st century. *Technovation*, *25*(6), 569-585.

[2] Rosli, R. E., Sulong, A. B., Daud, W. R. W., Zulkifley, M. A., Husaini, T., Rosli, M. I., ... & Haque, M. A. (2017). A review of high-temperature proton exchange membrane fuel cell (HT-PEMFC) system. *International Journal of Hydrogen Energy*, *42*(14), 9293-9314.

[3] N. Goria, «Analisi e modellazione delle prestazione di uno stack PEM di laboratorio- Politecnico di Torino,» 2023. [Online].

[4] Wang, Y., Pang, Y., Xu, H., Martinez, A., & Chen, K. S. (2022). PEM Fuel cell and electrolysis cell technologies and hydrogen infrastructure development–a review. *Energy & Environmental Science*, *15*(6), 2288-2328.

[5] «Modofluido,» [Online]. Available: https://modofluido.hydac.it/fuell-cell#:~:text=Le%20celle%20a%20combustibile%20sono,drogeno%20direttamente%20in%20energia%20elettrica. [Consultato il giorno 2023].

[6] «Wikipedia,» Wikipedia, [Online]. Available: https://it.wikipedia.org/wiki/Pila_a_combustibile_con_membrana_a_scambio_protonico. [Consultato il giorno 2023].

[7] «Wikipedia,» [Online]. Available: https://it.wikipedia.org/wiki/Nafion. [Consultato il giorno 2023].

[8] Mu'min, M. S., Komma, M., Abbas, D., Wagner, M., Krieger, A., Thiele, S., ... & Kerres, J. (2023). Electrospun phosphonated poly (pentafluorostyrene) nanofibers as a reinforcement of Nafion membranes for fuel cell application. *Journal of Membrane Science*, *685*, 121915.

[9] Marken, F., Carta, M., & McKeown, N. B. Polymers of Intrinsic Microporosity (PIMs) in the Design of Electrochemical Multi-Component and Multi-Phase Interfaces.

[10] Byun, G. H., Kim, J. A., Kim, N. Y., Cho, Y. S., & Park, C. R. (2020). Molecular engineering of hydrocarbon membrane to substitute perfluorinated sulfonic acid membrane for proton exchange membrane fuel cell operation. *Materials Today Energy*, *17*, 100483.

[11] S. D. M. W.-P. F. BAUER, *Wiley InterScience,* 2004.

[12] Han, W., Zhang, C., Zhao, M., Yang, F., Yang, Y., & Weng, Y. (2021). Post-modification of PIM-1 and simultaneously in situ synthesis of porous polymer networks into PIM-1 matrix to enhance CO2 separation performance. *Journal of Membrane Science*, *636*, 119544..

[13] F. Marken,E. Madrid, Y. Zhao, N.B. Mckeown, M. Carta «Polymers of Intrinsic Microporosity in Triphasic,» *ChemPubSoc,* 2019.

[14] McKeown, N. B. (2020). Polymers of intrinsic microporosity (PIMs). *Polymer*, *202*, 122736.

[15] E. Lasseuguette, M. Ferrari, S. Brandani « Humidity Impact on the Gas Permeability of PIM-1 Membrane for Post-combustion Application» December 2014. Available: https://www.researchgate.net/publication/270345037_Humidity_Impact_on_the_Gas_Permeability_of_PIM-1_Membrane_for_Post-combustion_Application.

[16] Li, Q. F., Rudbeck, H. C., Chromik, A., Jensen, J. O., Pan, C., Steenberg, T., ... & Kerres, J. (2010). Properties, degradation and high temperature fuel cell test of different types of PBI and PBI blend membranes. *Journal of Membrane Science*, *347*(1-2), 260-270.

[17] Olvera-Mancilla, J., Palacios-Alquisira, J., Escobar-Barrios, V. A., & Alexandrova, L. (2019). Some aspects of polybenzimidazoles' synthesis in Eaton reagent under different temperatures and microwave irradiation. *Journal of Macromolecular Science, Part A*, *56*(6), 609-617.

[18] Jespersen, J. L., Schaltz, E., & Kær, S. K. (2009). Electrochemical characterization of a polybenzimidazole-based high temperature proton exchange membrane unit cell. *Journal of Power Sources*, *191*(2), 289-296.

[19] «Mettler toledo» [Online]. Available: https://www.mt.com/it/it/home/applications/L1_AutoChem_Applications/ftir-spectroscopy/attenuated-total-reflectance-atr.html.

[20] «Wikipedia,» [Online]. Available: https://en.wikipedia.org/wiki/Attenuated_total_reflectance.

[21] PerkinElmer, «FT-IR Spectroscopy Attenuated Total Reflectance (ATR),» Perkin Elmer Life and Analytical Sciences, 16 Febbraio 2007. [Online]. Available: https://web.archive.org/web/20070216065646/http://las.perkinelmer.com/content/TechnicalInfo/TCH_FTIRATR.pdf.

[22] «Wikipedia,» [Online]. Available: https://en.wikipedia.org/wiki/Thermogravimetric_analysis.

[23] Infinitia, «Infinitiaresearch,» [Online]. Available: https://www.infinitiaresearch.com/en/sin-categoria-en/tga-what-is-thermogravimetric-analysis/. [Consultato il giorno 2023].

[24] A. Research, «Auriga research,» [Online]. Available: https://aurigaresearch.com/pharmaceutical-testing/thermogravimetric-analysis-tga/.

[25] «Wikipedia,» [Online]. Available: https://en.wikipedia.org/wiki/Differential_scanning_calorimetry. [Consultato il giorno 2023].

[26] Gill, P., Moghadam, T. T., & Ranjbar, B. (2010). Differential scanning calorimetry techniques: applications in biology and nanoscience. *Journal of biomolecular techniques: JBT*, *21*(4), 167.

[27] Hoogenboom, R., & Schubert, U. S. (2007). Microwave-assisted polymer synthesis: recent developments in a rapidly

expanding field of research. *Macromolecular Rapid Communications*, *28*(4), 368-386.

[28] Budd, P. M., Elabas, E. S., Ghanem, B. S., Makhseed, S., McKeown, N. B., Msayib, K. J., ... & Wang, D. (2004). Solution-processed, organophilic membrane derived from a polymer of intrinsic microporosity. *Advanced Materials*, *16*(5), 456-459.

[29] Yong, W. F., Li, F. Y., Chung, T. S., & Tong, Y. W. (2014). Molecular interaction, gas transport properties and plasticization behavior of cPIM-1/Torlon blend membranes. *Journal of Membrane Science*, *462*, 119-130.

[30] Du, N., Robertson, G. P., Song, J., Pinnau, I., Thomas, S., & Guiver, M. D. (2008). Polymers of intrinsic microporosity containing trifluoromethyl and phenylsulfone groups as materials for membrane gas separation. *Macromolecules*, *41*(24), 9656-9662.

[31] Du, N., Robertson, G. P., Song, J., Pinnau, I., & Guiver, M. D. (2009). High-performance carboxylated polymers of intrinsic microporosity (PIMs) with tunable gas transport properties. *Macromolecules*, *42*(16), 6038-6043.

[32] Merck, «Sigmaaldrich,» 2023. [Online]. Available: https://www.sigmaaldrich.com/GB/en/technical-documents/technical-article/analytical-chemistry/photometry-and-reflectometry/ir-spectrum-table. [Consultato il giorno 2023].

[33] Zannichelli, «Bande di assorbimento ir,» 11 01 2014. [Online]. Available: https://online.scuola.zanichelli.it/analisichimicastrumentale/files/2014/01/11_appendice_Bande-assorbimento-IR.pdf.

[34] Han, W., Zhang, C., Zhao, M., Yang, F., Yang, Y., & Weng, Y. (2021). Post-modification of PIM-1 and simultaneously in situ synthesis of porous polymer networks into PIM-1 matrix to enhance CO2 separation performance. *Journal of Membrane Science*, *636*, 119544..

[35] J. W. &. Sons, «Inc. SpectraBase,» [Online]. Available: https://spectrabase.com/spectrum/G4CBuKNSKtQ. [Consultato il giorno 24 7 2023].

[36] Olvera-Mancilla J, Palacios-Alquisira J, Alexandrova L. Eaton's reagent in polybenzimidazole synthesis: The influence of temperature and microwave irradiation. High Performance Polymers. 2018;30(6):699-709. doi:10.1177/0954008317716977.

[37] Mallakpour, S., & Dinari, M. (2012). Novel nanostructure amino acid-based poly (amide–imide) s enclosing benzimidazole pendant group in green medium: fabrication and characterization. *Amino Acids*, *43*(4), 1605-1613..

[38] Alvarez-Gallego, Y., Ruffmann, B., Silva, V., Silva, H., Lozano, A. E., de la Campa, J. G., ... & de Abajo, J. (2008). Sulfonated polynaphthalimides with benzimidazole pendant groups. *Polymer*, *49*(18), 3875-3883.

[39] Jung, D., Chen, Z., Alayoglu, S., Mian, M. R., Goetjen, T. A., Idrees, K. B., ... & Farha, O. K. (2021). Postsynthetically modified polymers of intrinsic microporosity (PIMs) for capturing toxic gases. *ACS Applied Materials & Interfaces*, *13*(8), 10409-10415.

[40] Maruccia, E., Lourenço, M. A., Priamushko, T., Bartoli, M., Bocchini, S., Pirri, F. C., ... & Gerbaldi, C. (2022). Nanocast nitrogen-containing ordered mesoporous carbons from glucosamine for selective CO2 capture. *Materials Today Sustainability*, *17*, 100089.